International Journal of Nanomedicine

Dovepress

open access to scientific and medical research

Open Access Full Text Article

ORIGINAL RESEARCH

Pairing 3D-Printing with Nanotechnology to Manage Metabolic Syndrome

Khalid M El-Say[1,2], Raed I Felimban[3,4], Hossam H Tayeb[4,5], Adeel G Chaudhary[3,6], Abdelsattar M Omar[7–9], Waleed Y Rizg[1,2], Fuad H Alnadwi[10], Fathy I Abd-Allah[11], Tarek A Ahmed[1,2]

[1]Department of Pharmaceutics, Faculty of Pharmacy, King Abdulaziz University, Jeddah, 21589, Saudi Arabia; [2]Center of Research Excellence for Drug Research and Pharmaceutical Industries, Pharmaceutical Technology Unit, King Abdulaziz University, Jeddah, 21589, Saudi Arabia; [3]Department of Medical Laboratory Sciences, Faculty of Applied Medical Sciences, King Abdulaziz University, Jeddah, 21589, Saudi Arabia; [4]Center of Innovation in Personalized Medicine (CIPM), 3D Bioprinting Unit, King Abdulaziz University, Jeddah, 21589, Saudi Arabia; [5]Center of Innovation in Personalized Medicine (CIPM), Nanomedicine Unit, King Abdulaziz University, Jeddah, 21589, Saudi Arabia; [6]Center of Innovation in Personalized Medicine (CIPM), King Abdulaziz University, Jeddah, 21589, Saudi Arabia; [7]Department of Pharmaceutical Chemistry, Faculty of Pharmacy, King Abdulaziz University, Jeddah, 21589, Saudi Arabia; [8]Department of Pharmaceutical Chemistry, Faculty of Pharmacy, Al-Azhar University, Cairo, 11884, Egypt; [9]Centre for Artificial Intelligence in Precision Medicines, King Abdulaziz University, Jeddah, Saudi Arabia; [10]Department of Nuclear Engineering, Faculty of Engineering, King Abdulaziz University, Jeddah, 21589, Saudi Arabia; [11]Department of Pharmaceutics and Industrial Pharmacy, Faculty of Pharmacy, Al-Azhar University, Cairo, 11651, Egypt

Correspondence: Khalid M El-Say, Department of Pharmaceutics, Faculty of Pharmacy, King Abdulaziz University, Jeddah, Saudi Arabia, Tel +966-58-293-4511, Fax +966 26951696, Email kelsay1@kau.edu.sa

Introduction: This work was aimed to develop a Curcuma oil-based self-nanoemulsifying drug delivery system (SNEDDS) 3D-printed polypills containing glimepiride (GMD) and rosuvastatin (RSV) for treatment of dyslipidemia in patients with diabetes as a model for metabolic syndrome (MS).

Methods: Compartmentalized 3D printed polypills were prepared and studied in streptozotocin/poloxamer induced diabetic/dyslipidemic rats. The pharmacokinetic parameters of GMD and RSV in the prepared polypills were evaluated. Blood glucose level, lipid profile, antioxidant, and biochemical markers activities were investigated. Also, histopathological examination of the liver and pancreas was carried out. The atherosclerotic index, the area of islets of Langerhans, and liver steatosis lesion scores were calculated.

Results: The developed SNEDDS-loaded GMD/RSV polypills showed acceptable quality control characteristics with a high relative bioavailability of 217.16% and 224.28% for GMD and RSV, respectively, when compared with the corresponding non-SNEDDS pills. The prepared polypills showed dramatic lowering in blood glucose levels and substantial improvement in lipid profile and hepatic serum biomarkers as well as remarkable decrease in serum antioxidants in response to Poloxamer 407 intoxication. The prepared polypills decreased the risk of atherosclerosis and coronary disease by boosting the level of high-density lipoprotein and lowering both triglyceride and low-density lipoprotein. Microscopic examination showed normal hepatic sinusoids and high protection level with less detectable steatosis in the examined hepatocytes. Normal size pancreatic islets with apparently normal exocrine acini and pancreatic duct were also noticed.

Conclusion: This formulation strategy clearly shows the potential of the developed polypills in personalized medicine for treatment of patients with MS.

Keywords: 3D-printed tablets, Curcuma oil, glimepiride, metabolic syndrome, rosuvastatin, SNEDDS, nanotechnology

Introduction

Metabolic syndrome (MS) is a collection of cardiometabolic risk factors that involve insulin resistance, abdominal obesity, hypertension, hyperglycemia, and dyslipidemia. MS increases the risks of cardiovascular disease (CVD), type 2 diabetes mellitus (T2DM), and all-cause mortality in the general population.[1,2] The overall prevalence of MS ranges from 20% to 25% in adults[2,3] and 0% to 19.2% in children,[4] but it can reach almost 80% in type 2 diabetes patients.[5,6] The most frequently observed component of MS was found to be low levels of high-density lipoprotein (HDL), followed by abdominal obesity. The incidence of MS often parallels the incidence of obesity and the incidence of type 2 diabetes (one of the outcomes of MS).[7]

Received: 27 January 2022
Accepted: 11 April 2022
Published: 21 April 2022

Graphical Abstract

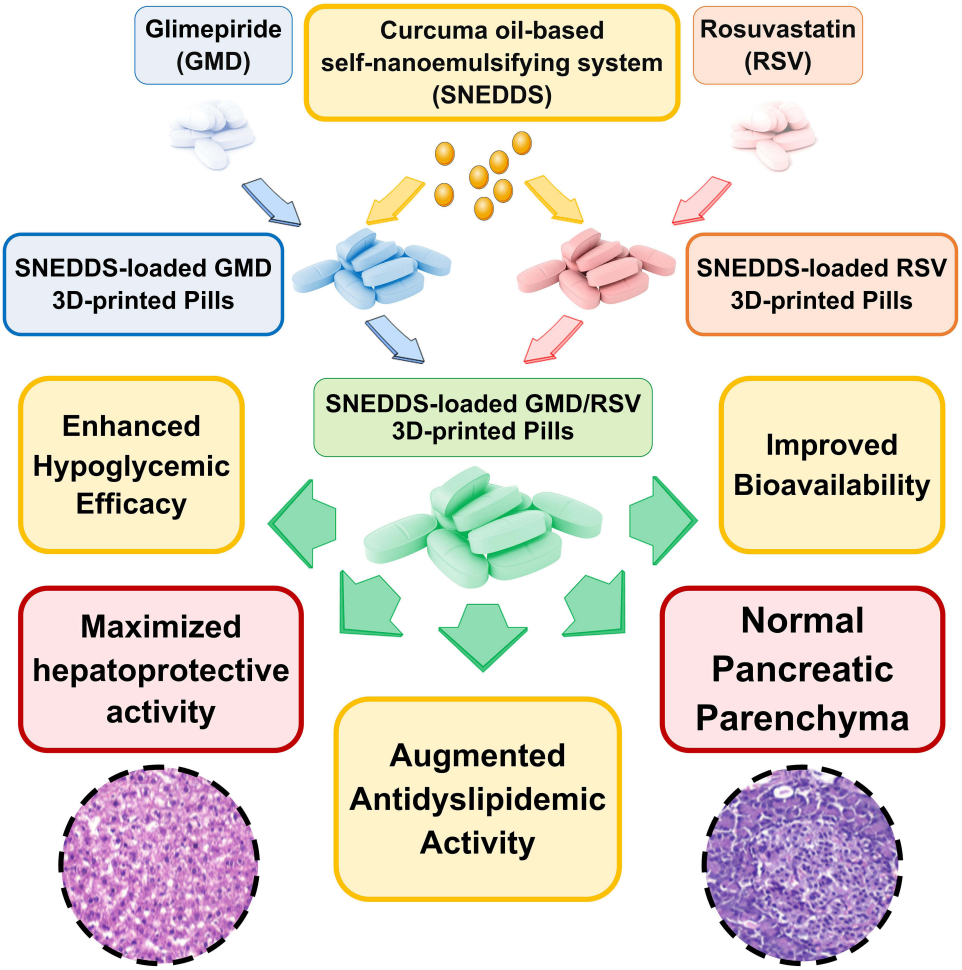

According to the National Cholesterol Education Program – Third Adult Treatment Panel (NCEP ATP III), a patient must have at least three of the five cardiovascular risk factors at the same time to be diagnosed with the syndrome. These risk factors include waist circumference; high triglyceride; lower HDL cholesterol; high blood pressure or previously diagnosed hypertension; high fasting plasma glucose (≥100 mg/dl) or previous diagnosis of type 2 diabetes.[2,8] According to the National Diabetes Statistics Report, a periodic publication of the Centers for Disease Control and Prevention (CDC) published in 2020, about 34.2 million people of all ages (10.5% of the US population) had diabetes. About 34.1 million adults aged 18 years or older (or 13.0% of all US adults) had diabetes. About 7.3 million adults aged 18 years or older who met laboratory criteria for diabetes were undiagnosed diabetes. This indicates that the percentage of adults with diabetes increased with age, reaching 26.8% among those aged 65 years or older. Also, the prevalence of prediabetes was about three times more. So, about one-third of US adults have MS.[9] Furthermore, the severity of MS is associated with a concomitant reduction in the risk of further T2DM and CVD.[10] Also, it is reported that nearly one-fourth of the type 1 diabetes patients were affected by MS.[11] To help in the management and treatment of MS, the development of multicompartmental pills with different technology approaches is urgently needed.

Development of a novel drug-loaded delivery system and implementing nanotechnology in drug delivery are useful in controlling and maintaining an adequate drug concentration in the target tissue. A plurality of examples implementing drug-loaded nanomaterials as efficient drug delivery systems is known in the art. For example, the use of

nanomaterials in personalized medicine is known to allow the tailoring of drug products to treat an individual patient or a group of related patients suffering a particular disease. Also, organic, and inorganic materials have been investigated as potential drug carriers in many medical applications. The interaction of inorganic minerals with amino acids, peptides, and proteins has made significant biological progress.[12] The potential actions of drug loaded inorganic nanoparticles have outperformed traditional chemotherapy medications, particularly in the treatment of cancer.[13–15] Furthermore, inorganic nanoparticles may have the potential to enhance neurodegenerative disorders and other diseases.[16] Organic materials' outstanding function in medicine continues to be one of the most important factors in the drug development process.[17] Metal–organic frameworks on a nanoscale have been investigated as drug delivery and imaging carriers.[18]

Over the last decades, there is a growing interest in Curcuma oil/curcumin due to its roles in the treatment of MS by adjusting the parameters triggered by the metabolic disorders and eliminating its negative effects.[19] Moreover, it has potential in the treatment of cardiovascular disorders which include lowering the total blood cholesterol and low-density lipoprotein levels.[20] Also, it improves the metabolic profile of patients with diabetes mellitus mainly concerning lipid levels, and reduces the associated complications.[21] Interestingly, the clinical data supported the safety of Curcuma oil/curcumin and recommended unlocking the potential of this polyphenol as a preventive and/or therapeutic strategy for statin-associated muscle symptoms (SAMS). This is due to its effect in the improvement of mitochondrial function, along with analgesic, anti-inflammatory, antioxidant, and lipid-modifying properties which supports the potential advantage of curcumin supplement as an adjunct to statin therapy in patients with SAMS, as well as in persons with a residual cardiovascular risk.[22] In addition, the administration of Curcuma oil/curcumin increases the basal metabolic rate and releases some cytokines that can reduce body weight. Also, it reduces hepatic fat accumulation and prevents steatosis by downregulating lipogenic factors. In addition, it improves insulin sensitivity and glycemic control and reduces the biomarkers of systemic inflammation, hepatocyte injury, and oxidative stress. Interestingly, it is noticed that nano-formulation of curcumin significantly reduced total cholesterol, triglycerides, serum lipoproteins, serum C reactive protein, and plasma malonaldehyde. So, it can be deemed in the therapeutic approach of patients with MS.[23]

Patients who have huge variations like those of MS need tailored therapy to ensure better medical care. Of note, three-dimensional (3D) printing technology has been considered as a useful drug delivery manufacturing system in that a 3D structure can be manufactured by fusing or depositing different materials through applying the strategy of layer-by-layer additive manufacturing. Patient-specific 3D-printed medications are becoming increasingly beneficial in personalized treatments. Personalized medicine aims to ensure better health care with much lower cost by selecting the most appropriate and ideal therapy for individual patients. Also, personalized medicine is usually designed for patients that are suffering from genetic variations or not responding to the traditional health system, which necessitates providing tailored drug prescriptions and/or changes in the therapeutic practice manners and strategies of the health care professionals.[24,25]

Despite the advantageous features of the current 3D printed medications, several factors may be of concern to the effectiveness of the 3D printed drug delivery system. For example, many active pharmaceutical ingredients (APIs) do not reach the commercialization step due to their limited oral bioavailability. Another important current problem in the pharmaceutical industry for drugs of limited bioavailability is mainly attributed to their inadequate aqueous solubility and dissolution rate. Moreover, a high percentage of the administered drug is lost during the absorption process due to the first-pass metabolism phenomenon. Thus, there is a need for a composition and a method for providing an improved 3D printed drug-delivering tablet with increased aqueous solubility and dissolution rate for ease of bioavailability. For these reasons, a combination of 3D printing technology and nanotechnology was employed in this study to print tablets containing a mixture of glimepiride (GMD) and rosuvastatin (RSV) with curcuma oil after forming them into a self-nanoemulsifying system to improve their absorption and bioavailability. As a result, this formulation of 3D-printed polypills containing nanosized drugs can be customized to each patient with MS. Also, in this work, the pharmacokinetics, hyperglycemic/dyslipidemic activities, and histopathological changes of Curcuma oil-based self-nanoemulsifying drug delivery system (SNEDDS) 3D printed polypills containing GMD and RSV were investigated. Moreover, the atherosclerotic index, the area of islets of Langerhans, and liver steatosis lesion scores

were calculated to investigate the potential of the developed polypills in personalized medicine for treatment of patients with MS.

Materials and Methods

Materials

Glimepiride was obtained as gift samples from the Saudi Pharmaceutical Industries & Medical Appliances Corporation (SPIMACO) (Al Qassim, Saudi Arabia). Rosuvastatin was kindly gifted by and the Saudi Arabian Japanese Pharmaceuticals Co. Ltd (SAJA) (Jeddah, Saudi Arabia). Microcrystalline cellulose (Avicel) PH-101 was purchased from Winlab laboratory chemicals (Leicestershire, UK). Hydroxypropyl methylcellulose (HPMC) 4000 cp were obtained from Spectrum Chemical Manufacturing Corporation (Gardena, CA). Lactose anhydrous, Polyethylene glycol (PEG) 400, Tween 80, Polyvinyl pyrrolidone (PVP) with a molecular weight of 360,000 Da (K90), Methocel® A15 LV, 27.5–31.5% methoxyl basis, acetonitrile, and methanol were purchased from Sigma-Aldrich Inc. (St. Louis, MO). Croscarmellose sodium (Ac-Di-Sol) from Biosynth International, Inc (San Diego, CA).

Preparation and Characterization of Curcuma Oil-Based SNEDDS

To our knowledge, the Curcuma oil-based SNEDDS has been prepared, evaluated and optimized in the first part of this work that has been previously published in Ahmed et al.[26] Briefly, an optimized Curcuma oil-based self-nanoemulsifying drug delivery system (SNEDDS) formulation was prepared in a screw cap vial by mixing the accurate weights of *Curcuma longa* oil (15%), Tween 80 (10%), and PEG 400 (75%) using vortex for 60s to get a homogenous dispersion.

To evaluate the size and polydispersity index (PDI) of the prepared SNEDDS, 1g was added to 10 mL of distilled water on a magnetic stirrer until a homogenous yellowish nanoemulsion was obtained. The size and PDI of the obtained emulsion were analyzed using Malvern Zetasizer Nano ZSP, Malvern Panalytical Ltd. (Malvern, UK).

Preparation and in vitro Characterization of 3D-Printed Polypills

To the best of our knowledge, the 3D-printed polypills have been prepared, and characterized in the first part of this work that has been previously published in Ahmed et al.[26] To develop medicated 3D-printed polypills, hydroxypropyl methylcellulose gel pastes were first prepared. SNEDDS-based gel pastes and non-SNEDDS gel pastes loaded with either GMD or RSV were prepared. Non-SNEDDS gel pastes were prepared by dispersing the known weight of GMD or RSV to a specified volume of distilled water over a magnetic stirrer and 4% of HPMC was added. Stirring was continued until homogenous gels were obtained that were kept in the refrigerator for 24 h at 4°C for complete swelling of the polymer. Gels containing the optimized SNEDDS formulation were prepared by dispersing the specified weight of GMD or RSV in 2 g of SNEDDS and adding the medicated SNEDDS to 18 mL of distilled water on a magnetic stirrer. Finally, HPMC (4%) was added with continuous stirring and the mixtures were left in the refrigerator. Plain (drug-free) SNEDDS-based gel formulation was also prepared with the same procedure to be used as a control in the assessment of pharmacodynamic activity.

Different tablet excipients were added to the prepared gels to develop pastes suitable for tablet printing. Avicel (20% w/w) as an insoluble ingredient, lactose (10% w/w) and Methocel (5% w/w) as adsorbent for the SNEDDS formulation, PVP K90 (10% w/w) as a binder, and Ac-Di-Sol (5% w/w) as a disintegrant was gradually mixed to the prepared gels in a mortar until a homogenous paste was obtained. Five different paste formulations were prepared namely, plain (non-medicated) SNEDDS-loaded paste, non-SNEDDS-loaded GMD paste, non-SNEDDS-loaded RSV paste, SNEDDS-loaded GMD paste, and SNEDDS-loaded RSV paste. The flow properties and viscosity values of the prepared pastes were studied using a Kinexus oscillation rheometer (Malvern Instruments Ltd. Worchestershire, UK).

Three-dimensional printed (3D-P) pills were developed from the prepared pastes utilizing REGEMAT3D V1 BioPrinter (REGEMAT Inc. Granada, Spain). A computer-aided design modeling software (REGEMAT 1.4.9 Designer) was used during the printing process. Each paste formulation was loaded into the extrusion tool and extruded through a 0.58 mm printing nozzle. The flow speed was adjusted at 2.6 mm/s and the infill speed was 10 mm/s. Printing was done layer-by-layer in a horizontal and vertical direction at room temperature. For each formulation, a total of eight

layers were printed in the selected area of the building plate to develop a cylinder of 15 mm diameter. The printing process was conducted for the prepared five gel paste formulations. Another multi-compartment tablet (polypill) formulation was printed utilizing eight layers of the paste containing GMD and eight layers of the paste containing RSV. All the printed tablet formulations were dried in a vacuum dryer at 40°C for 24 h and finally kept in a hermetically sealed container. The quality attributes of the prepared tablets were evaluated according to the specification stated in the United States Pharmacopeia.[27]

In vivo Studies on the Induced Hyperglycemic/Dyslipidemic Rats

Pharmacokinetics Evaluation

Study Design and Animal Handling

A single dose one-period parallel design was used to study the pharmacokinetics of GMD and RSV from the prepared 3D-P polypills (F2-F6). Male Wistar rats of an average weight of 200–250 g were used. Normal animals without treatment were used as a control. Diabetes was induced in the studied animals by intraperitoneal injection of 50 mg/kg streptozotocin two weeks before the study. Fasting blood glucose level was assessed using All Medicus GlucoDr SuperSensor Device (AGM-2200), All Medicus Co. Ltd., (Gyeonggi-do, REPUBLIC of KOREA). Rats having moderate diabetes, with fasting blood glucose levels in the range of 200–300 mg/100 mL, were selected. Hyperlipidemia was induced in animals by intraperitoneal injection of 0.25 g/kg Poloxamer 407 dissolved in 0.9% saline, 24 h before drug administration. Animals with hyperlipidemia and hyperglycemia were classified into six groups (6 per each). Group, I was assigned as a control group while group II was assigned for animals with induced hyperlipidemia and hyperglycemia without treatment (model group). Group III, IV, V, VI, and VII were administered tablet formulations F1, F2, F3, F4, and F5. Before animal treatment, rats were kept in a temperature-controlled closed area with a 12 h light/darkness cycle for one week with free access to water and food. GMD dose of 10 mg/kg and RSV dose of 20 mg/kg were used.[28,29] Each 3D-P tablet formulation was crushed and suspended in an aqueous solution of carboxymethyl cellulose (1%) to prepare a uniform suspension suitable for oral administration through a gastric tube. Blood samples were collected through retro-orbital puncturing over 24 h for animals treated with GMD and extended to 72 h for animals treated with RSV. The plasma was immediately separated from the blood samples by centrifugation at 6000 rpm for 10 min and stored frozen at −20°C until analysis. The protocol for this study was approved by the Research Ethics Committee, Faculty of Pharmacy, King Abdulaziz University, SA (Reference No. 1021442). The study was conducted according to the guidelines of Good Clinical Practice, the International Conference on Harmonization, and the European Medicines Agency.

Chromatographic Conditions

Calibration curves for GMD and RSV were constructed from blank rat plasma samples. For the determination of GMD, a methanolic stock solution of metformin was used as an internal standard. The plasma GMD concentration in the unknown and the prepared calibration standards was determined using Perkin Elmer high-performance liquid chromatography (HPLC) equipped with variable wavelength UV detector and autosampler. Phenomenex, RP Hi-Q-Sil C18 column (250 × 4.6 mm, 5 µm, Phenomenex Inc.) was used for separation. The mobile phase consisted of 64:36 acetonitrile and 0.02 M potassium dihydrogen orthophosphate adjusted to pH 3.5. The injection volume used was 30 µL with a flow rate of 1 mL/min. The UV detector was adjusted at 230 nm. For extraction and preparation of the samples; 1 mL of acetonitrile-methanol (1:1) mixture was added to each sample. The mixture was vortexed for 1 min and centrifuged for 10 min at 5000 rpm. The organic phase was separated and evaporated to dryness under a constant stream of nitrogen at 50°C. The residue was reconstituted in 80 µL of the mobile phase and a volume of 30 µL was injected. The condition employed for quantification of GMD in the plasma samples was conducted as previously mentioned except for slight modification.[30]

For RSV determination, atorvastatin was used as an internal standard. Quantification of RSV in the calibration standards and the unknown samples was done using the same apparatus and condition mentioned above for GMD except that the mobile phase consisted of acetonitrile and 0.1% phosphoric acid (58:42) and the UV detector was adjusted at 240 nm. Extraction and separation of RSV were achieved as described above for GMD except that the residue was reconstituted in 80 µL of acetonitrile and 0.1% phosphoric acid (58:42). The method used for the analysis of RSV in the plasma samples utilized the

condition previously reported by Ahmed et al.[29] PK solver (An add-in program for pharmacokinetic data) was utilized to calculate the pharmacokinetic parameters using the non-compartmental extravascular pharmacokinetic model. Maximum plasma drug concentration (C_{max}), time to reach the maximum plasma drug concentration (T_{max}), the area under the plasma drug concentration-time curve to the last time point (AUC_{0-t}) and infinity (AUC_{0-inf}), the elimination rate constant (Lambda_z), the mean residence time (MRT), elimination half-life ($t_{½}$), total body clearance (Cl/F) and the apparent volume of distribution (Vz/F).

Pharmacodynamics Study (Hypoglycemic and Antidyslipidemic Effects)

The blood glucose level (BGL) in the studied animals was measured over 24 h after administration of a single oral dose of 10 mg/kg GMD formulations by intragastric tubing. Blood samples were collected through retro-orbital puncturing from groups of animals administered GMD formulations compared with the group of animals that received the plain Curcuma oil-loaded SNEDDS over 24 h.

The antidyslipidemic activity was evaluated in the groups of animals those administered RSV formulations compared with the group of animals that received the plain Curcuma oil-loaded SNEDDS over 72 h. Serum was separated by keeping the collected blood samples for 1 h in centrifuge tubes, to allow clotting, followed by centrifugation for 15 min at 3000 rpm. The separated serum samples were assessed for total cholesterol, triglycerides (TG), low-density lipoproteins (LDL), and high-density lipoproteins (HDL) using (Colorimetric/Fluorometric) Assay Kit (ab65390) which provides a simple quantification method of the studied parameters after convenient separation of the different lipoprotein fractions.

Hepatoprotective and Antioxidant Activities

The liver function of the studied animals was evaluated before and after treatment by assessing the serum levels of aspartate aminotransferase (AST), alanine aminotransferase (ALT), and alkaline phosphatase (ALP) enzymes. The concentrations of these enzymes were measured using the colorimetric method utilizing Spectrum diagnostic ALT, AST, and ALP reagents of the Egyptian company for biotechnology (Cairo, Egypt). The reagents were supplied ready-to-use and they are used only with non-haemolyzed serum samples. Heparin and EDTA are the only acceptable anticoagulants. Measurement was performed at 546 nm at a sample: reagent ratio of 1: 60.

Also, the antioxidant activity was studied by monitoring the serum levels of catalase (CAT), glutathione transferase (GST), and superoxide dismutase (SOD) enzymes. CAT and SOD serum concentrations were measured using colorimetric assay kits of Bio-diagnostic (Giza, Egypt), catalog # CA 25 17 and SD 25 21 for CAT and SOD, respectively. GST was quantified using rat Glutathione S-transferase (GSTs) ELISA Kit (Catalog # MBS260372).

Histopathological Examination of Liver and Pancreas Tissues

The animals under the study were sacrificed and the liver and pancreas specimens were taken and treated with 10% neutral buffer formalin. Paraffin sections were prepared at the desired thickness using a microtome and stained with hematoxylin and eosin. Finally, any changes in the tissues of the pancreas and liver were microscopically investigated.[31] Histopathological lesion of the liver samples was examined for steatosis following the criteria of Brunt et al.[32] Briefly, macro-vesicular steatosis was graded 0–3 based on the percent of hepatocytes in the biopsy (0 is none; 1 is up to 33%; 2 is 33–66%; 3 is > 66%); zonal distribution of steatosis and the presence of microvesicular steatosis were noted. Also, the area of islets of Langerhans was microscopically examined in the pancreas specimens of the investigated groups to assess the potential of 3D-P polypills in the protection of pancreas tissue.

Statistical Analysis

GraphPad Prism 8 software (GraphPad Inc., La Jolla, CA, USA) was used for the statistical analysis of the data for the pharmacokinetics of GMD and RSV. The data were expressed as mean ± SD and in the plasma concentration-time curve and two-way ANOVA followed by Tukey's multiple comparisons test was used to compare each means with the other at all time points to assess the significance between groups. The biochemical parameters were also assessed for their statistical difference using the two-way ANOVA followed by Tukey's multiple comparisons test, as well as a two-tailed

unpaired *t*-test was used to assess the difference between the biochemical parameters of the normal and model groups. Results with $P < 0.05$ were considered significant.

Results and Discussion

Development of SNEDDS

Based on its importance, Curcuma oil was used to develop SNEDDS with Tween 80 as a surfactant and PEG 400 as a cosurfactant. An optimized SNEDDS formulation that contains 15%, 10%, and 75% of Curcuma oil, surfactant, and cosurfactant respectively was prepared and showed the particle size and PDI values of 94.43 nm and 0.544, respectively.

Preparation and Characterization of 3D-Printed Polypills

All the prepared pastes exhibited a shear-thinning behavior of a pseudoplastic flow type. The obtained values for the viscosity of the studied pastes were 6550 ± 278, 8604 ± 295, 9185 ± 153, 6648 ± 135 and 6684 ± 451 Pa.s. The presence of the Curcuma oil-based SNEDDS in formulations leads to lower viscosity values due to lubrication of the solid particles and prevention of water loss from the paste. The obtained dried pills were cylindrical in shape and exhibited an acceptable weight, thickness and diameter. GMD containing pills demonstrated a drug content of not less than 98.0% while RSV containing pills illustrated a drug content of not less than 96.9% of the drug loading. Drug loading was found to range between 96.9% and 99.5%, which is within the acceptable range for content uniformity (85–115%) set by the British Pharmacopoeia. Also, the 3D-printed polypills demonstrating high reproducibility in physical dimensions, along with high mechanical strength resistant to damage on handling as indicated from the friability value which was less than 1%. The composition and characteristics of the prepared 3D-printed polypills are summarized in Table 1.

Assessment of Pharmacokinetic Parameters

Figure 1A depicted the plasma concentration-time profiles for the SNEDDS-loaded GMD pills and SNEDDS-loaded GMD/RSV pills in comparison to non-SNEDDS-loaded GMD pills after a single oral administration of 10 mg/kg of body weight for the induced-hyperglycemic/dyslipidemic male Wistar rats. The figure and the two-way ANOVA showed the significant difference (*p*-value <0.05) between the SNEDDS-loaded pills and the non-SNEDDS-loaded ones at all the time points of the study. The calculated values of the pharmacokinetic parameters for GMD from the investigated formulations are summarized in Table 2. The results revealed that the loading of GMD in the Curcuma oil-based SNEDDS hasten the absorption of the drug to reach its maximum plasma concentration (C_{max}) after 2 h instead of 4 h in the case of non-SNEDDS-loaded 3D-P pills. Compared with non-SNEDDS-loaded 3D-P pills, the C_{max} of GMD for SNEDDS-loaded GMD 3D-P pills and SNEDDS-loaded GMD/RSV 3D-P polypills were improved by more than 2 times. Also, SNEDDS-loaded GMD 3D-P pills and SNEDDS-loaded GMD/RSV 3D-P polypills showed a significantly higher area under the curve (16,263.25 ± 459.36 and 16,035.25 ± 371.43 ng/mL × h), respectively in comparison to the

Table 1 Composition and Characteristics of the Prepared 3D-Printed Polypills

	F1	F2	F3	F4	F5	F6
Drug	–	GMD	RSV	GMD	RSV	GMD and RSV
Drug loading (mg)	–	4	10	4	10	4 and 10
Weight after drying (mg)	532.58 ± 23.7	490.53 ± 27.76	498.88 ± 55.32	541.68 ± 61.02	559.39± 41.45	1067.54 ± 77.32
Thickness (mm)	3.035 ± 0.038	2.647± 0.160	2.826± 0.228	3.239 ± 0.178	2.876 ± 0.128	5.797 ± 0.156
Diameter (mm)	14.656 ± 0.148	13.289 ± 0.485	15.201 ± 0.228	14.855 ± 0.319	14.082 ± 0.249	14.342 ± 0.109
Friability (%)	0.068	0.159	0.199	0.117	0.043	0.089
Drug content (mg)	–	3.98± 0.201	9.76 ± 0.359	3.918 ± 0.219	9.691 ± 0.594	4.052± 0.087 and 9.711± 0.097

Abbreviations: GMD, glimepiride; RSV, rosuvastatin.

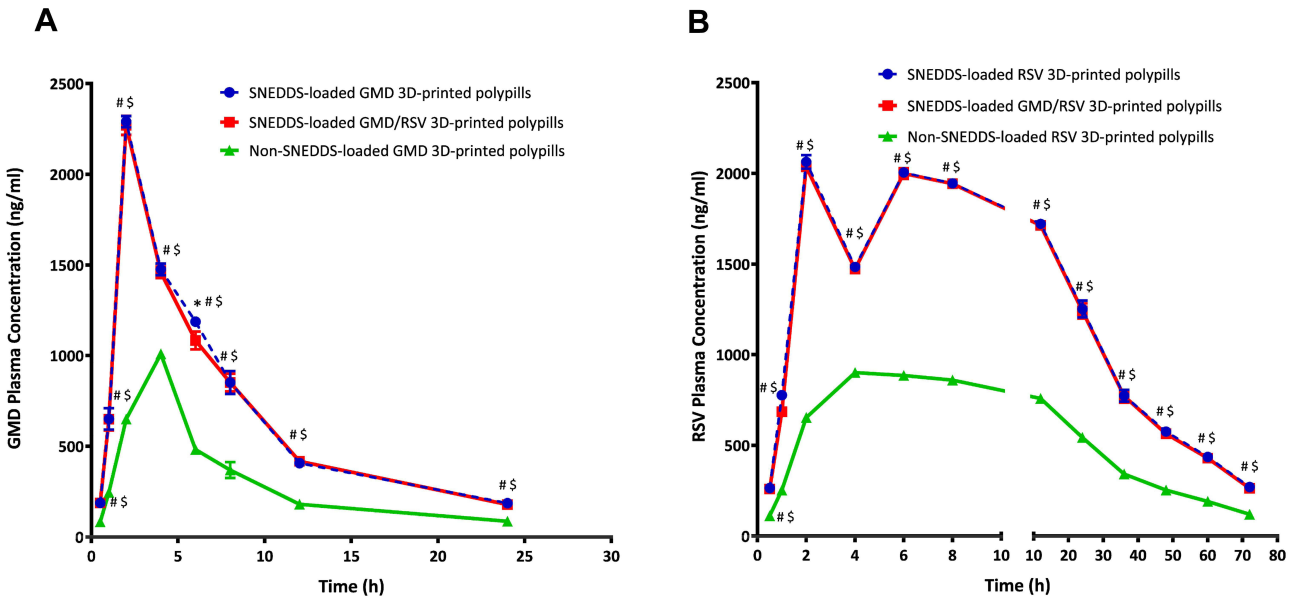

Figure 1 Plasma concentration-time curves for (**A**) GMD and (**B**) RSV after oral administration of the 3D-printed polypills to induced-hyperglycemic/dyslipidemic male Wistar rats. #Indicates significant difference between SNEDDS-loaded GMD 3D-P pills and non-SNEDDS-loaded 3D-P pills. $Indicates significant difference between SNEDDS-loaded GMD/RSV 3D-P pills and non-SNEDDS-loaded 3D-P pills. A significant difference was considered at $P < 0.05$. Data are presented as mean ± SD, (n = 6).

non-SNEDDS-loaded 3D-P pills (7,245.83 ± 386.63 ng/mL × h) which reflected on the significant increase in the relative bioavailability with 219.75% and 217.16%, respectively.

The same behavior was achieved in the plasma concentration-time profiles for the SNEDDS-loaded RSV pills and SNEDDS-loaded GMD/RSV pills in comparison to non-SNEDDS-loaded RSV pills after a single oral administration of 20 mg/kg of body weight for the induced-hyperglycemic/dyslipidemic male Wistar rats as depicted in Figure 1B. The plasma concentrations of RSV of SNEDDS-loaded RSV pills and SNEDDS-loaded GMD/RSV pills were significantly (*p*-value

Table 2 Pharmacokinetic Parameters of GMD After Oral Administration of 10 mg/kg in Rats (n = 6, the Data Expressed as Mean ± SD)

Parameter	Unit	Non-SNEDDS-Loaded GMD Pills	SNEDDS-Loaded GMD Pills	SNEDDS-Loaded GMD/RSV Pills
Lambda_z	1/h	0.09 (± 0.00)	0.11 (± 0.01)	0.10 (± 0.00)
$t_{1/2}$	h	7.49[a, b] (± 0.18)	6.36 (± 0.41)	6.68 (± 0.14)
T_{max}	h	4.00[a, b] (± 0.00)	2.00 (± 0.00)	2.00 (± 0.00)
C_{max}	ng/mL	1,008.67[a, b] (± 23.29)	2,290.33 (± 31.39)	2,270.00 (± 52.43)
AUC $_{0-t}$	ng/mL*h	7,245.83[a, b] (± 386.63)	16,263.25 (± 459.36)	16,035.25 (± 371.43)
AUC $_{0-inf}$	ng/mL*h	8,178.36[a, b] (± 419.23)	17,971.77 (± 562.95)	17,759.83 (± 337.25)
AUMC $_{0-inf}$	ng/mL*h^2	87,046.63[a, b] (± 5,116.42)	176,440.39 (±10,605.80)	176,286.42 (± 1,884.49)
MRT $_{0-inf}$	h	10.64 (± 0.21)	9.81 (± 0.35)	9.93 (± 0.17)
Vz/F	(mg)/(ng/mL)	0.01 (± 0.00)	0.01 (± 0.00)	0.01 (± 0.00)
Cl/F	(mg)/(ng/mL)/h	0.00 (± 0.00)	0.00 (± 0.00)	0.00 (± 0.00)
F	%	–	219.75	217.16

Notes: [a] Significantly different from values of SNEDDS-loaded GMD pills with *p*-value <0.05. [b] Significantly different from values of SNEDDS-loaded GMD/RSV pills with *p*-value <0.05.

Table 3 Pharmacokinetic Parameters of RSV After Oral Administration of 20 mg/kg in Rats (n = 6, the Data Expressed as Mean ± SD)

Parameter	Unit	Non-SNEDDS-Loaded RSV Pills	SNEDDS-Loaded RSV Pills	SNEDDS-Loaded GMD/RSV Pills
Lambda_z	1/h	0.03 (± 0.00)	0.03 (± 0.00)	0.03 (± 0.00)
$t_{1/2}$	h	23.20 (±0.28)	23.02 (± 0.22)	22.79 (± 0.15)
T_{max}	h	4.00[a, b] (± 0.00)	2.00 (± 0.00)	2.00 (± 0.00)
C_{max}	ng/mL	901.00[a, b] (± 10.00)	2,062.00 (± 38.30)	2,036.67 (± 22.50)
AUC $_{0-t}$	ng/mL*h	30,085.67[a, b] (± 645.03)	68,414.25 (± 1,461.16)	67,811.75 (± 1,470.46)
AUC $_{0-inf}$	ng/mL*h	34,101.93[a, b] (± 783.83)	77,371.16 (±1,811.78)	76,482.63 (± 1,678.71)
AUMC $_{0-inf}$	ng/mL*h^2	1,175,344.38[a, b] (± 36,253.05)	2,652,298.87 (± 84,867.52)	2,600,769.10 (± 70,329.74)
MRT $_{0-inf}$	h	34.46 (± 0.31)	34.28 (± 0.30)	34.00 (± 0.18)
Vz/F	(mg)/(ng/mL)	0.02 (± 0.00)	0.01 (± 0.00)	0.01 (± 0.00)
Cl/F	(mg)/(ng/mL)/h	0.00 (± 0.00)	0.00 (± 0.00)	0.00 (± 0.00)
F	%	–	229.88	224.28

Notes: [a]Significantly different from values of SNEDDS-loaded RSV pills with *p*-value <0.05. [b]Significantly different from values of SNEDDS-loaded GMD/RSV pills with *p*-value <0.05.

<0.05) higher than those of non-SNEDDS-loaded RSV pills at all the time points of the study. The calculated values of the pharmacokinetic parameters for RSV from the investigated formulations are summarized in Table 3. The t_{max} was 2 h in the SNEDDS-loaded RSV 3D-P pills instead of 4 h in the case of non-SNEDDS-loaded 3D-P pills. Also, the value of C_{max} for the SNEDDS-loaded RSV 3D-P pills and SNEDDS-loaded GMD/RSV 3D-P polypills were 2,062.00 ± 38.30 ng/mL and 2,036.67 ± 22.50 ng/mL, respectively versus 901.00 ± 10.00 ng/mL for non-SNEDDS-loaded 3D-P pills. Also, SNEDDS-loaded RSV 3D-P pills and SNEDDS-loaded GMD/RSV 3D-P polypills showed significance higher area under the curve (AUC_{0-t}) of 68,414.25 ± 1,461.16 and 67,811.75 ± 1,470.46 ng/mL×h, respectively in comparison to the non-SNEDDS-loaded 3D-P pills (30,085.67 ± 645.03 ng/mL×h). These findings reflected the significant increase in the relative bioavailability of RSV from the SNEDDS-loaded RSV 3D-P pills and SNEDDS-loaded GMD/RSV 3D-P polypills were 219.75% and 217.16%, respectively compared with that of non-SNEDDS-loaded 3D-P pills.

The plasma concentration-time profile following a single oral dose of SNEDDS-loaded RSV showed two separate peaks the first at 2 h and the second at 6 h which is known as the Double Peak Phenomenon. This phenomenon is explained by either enterohepatic recirculation, delayed gastric emptying, and/or variability of absorption.[33] In enterohepatic recirculation, the first peak in the profile is often the largest of the two peaks which were observed in our case with RSV loaded-SNEDDS. This phenomenon is attributed to the circulation of bile from the liver to the small intestine, where it promotes the digestion of fats and other substances and back to the liver which is in full agreement with the reported enhanced bioavailability of silymarin SMEDDS.[34] Also, the absence of the double peaks after oral administration of non-SNEDDS-loaded RSV formulation may be useful to negate the variability of absorption or the presence of two absorption sites along the gastrointestinal tract.[35]

The obtained results suggest that the incorporation of GMD and RSV in Curcuma oil-based SNEDDS with minimum globule size, loading onto 3D-P pills lead to an increase in the rate and extent of absorption as well as improving the oral bioavailability of these drugs which is in agreement with the previously reported results.[29,31,36–38] This improvement will be assessed and confirmed by the biochemical analysis of blood glucose level, TC, TG, HDL, and LDL as well as the calculation of the atherosclerotic index (AI), as a marker of cardiovascular disease.

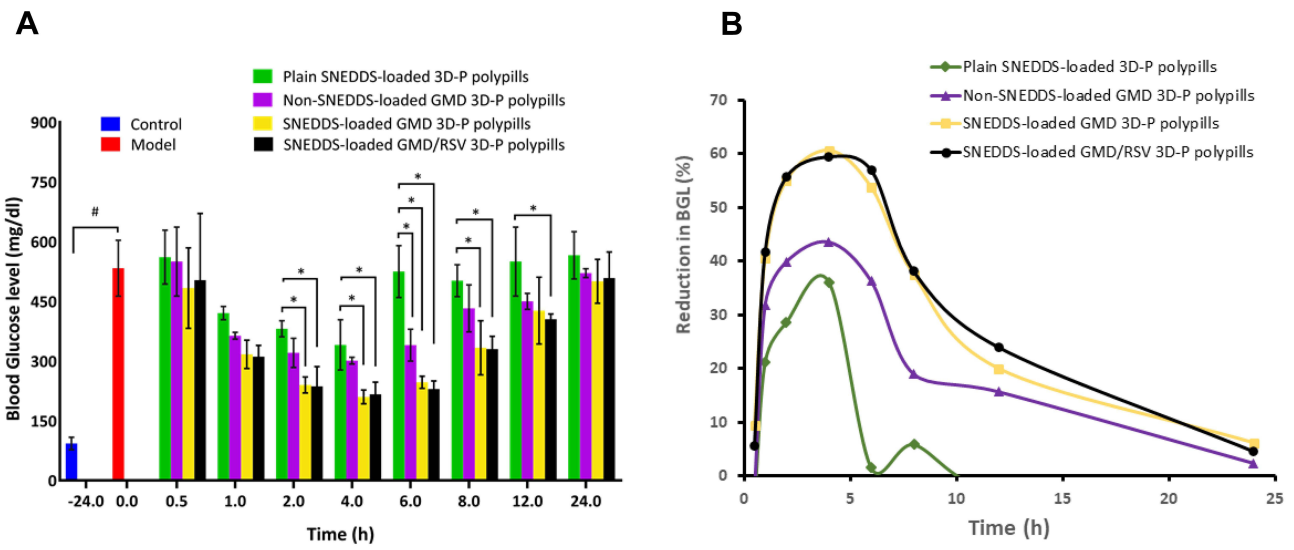

Figure 2 (**A**) Blood glucose level and (**B**) the percentage of inhibition of blood glucose level after oral administration of the 3D-printed polypills to induced-hyperglycemic /dyslipidemic male Wistar rats.

Notes: #Indicates significant from the control group. *Indicates significant from plain SNEDDS-loaded 3D-P pills. Significant difference was considered at $P < 0.05$. Data are presented as mean ± SD, (n = 3).

Assessment of Hypoglycemic Efficacy

There is a significant increase ($p < 0.05$) in BGL in the induced-hyperglycemic rats (model) when compared with the normal rats (control) as depicted in Figure 2A. This finding confirms the induction of diabetes in the rats after intraperitoneal injection of 50 mg/kg streptozotocin two weeks before the study. It is noticed that the plain SNEDDS-loaded pills containing only Curcuma oil showed a slight reduction in BGL over 4 h compared with the model group. Also, a significant reduction in BGL was noticed after administration of non-SNEDDS-loaded GMD pills that extended only for 6 h and then substantially increased. The hypoglycemic efficacy of SNEDDS-loaded GMD pills and SNEDDS-loaded GMD/RSV pills have shown a significant reduction ($p < 0.05$) after 1 h and extended to 8 h after administration. This significant reduction appeared in comparison with the model group and plain SNEDDS-loaded pills. On the other hand, there is no significant difference between SNEDDS-loaded GMD pills and SNEDDS-loaded GMD/RSV pills. Figure 2B revealed a percentage reduction of BGL after administration of a single dose of SNEDDS-loaded GMD pills or SNEDDS-loaded GMD/RSV pills of ~40% after 1 h and ~60% after 4 h and this reduction was extended for 8 h with ~40% from the model group. On the other hand, non-SNEDDS-loaded GMD pills showed a percentage reduction in BGL from 30% to 40% for not more than 6 h. This indicates that the duration of action of the SNEDDS-loaded formulations is markedly longer than that of the non-SNEDDS-loaded formulations.

Assessment of Antidyslipidemic Efficacy

The efficacy of the Curcuma oil SNEDDS-loaded GMD/RSV 3D-P polypills on the serum total cholesterol, triglyceride, HDL, and LDL was assessed in the induced-dyslipidemic rat model. The observed levels of the circulating lipids were significantly increased ($p < 0.05$) following oral administration of poloxamer 407 (Figure 3) which confirms the induction of hyperlipidemia in the model rats compared with the normal rats. Also, the figure revealed that there is a reduction in the total cholesterol, triglyceride, and LDL with ~27%, ~50%, and ~45%, respectively, after 24 h of the administration of the Curcuma oil-based SNEDDS-loaded 3D-P pills. The same behavior with a slight and insignificant difference has appeared with the non-SNEDDS-loaded RSV 3D-P pills. This finding displayed a hypolipidemic activity of Curcuma oil that is only loaded in the first formula and equivalent to the second formula that contains non-SNEDDS-loaded RSV. Figure 3A revealed that after 24 h, the SNEDDS-loaded RSV 3D-P pills and SNEDDS-loaded GMD/RSV 3D-P polypills significantly reduced the serum total cholesterol by ~46% and ~51%, respectively, which was significantly different from

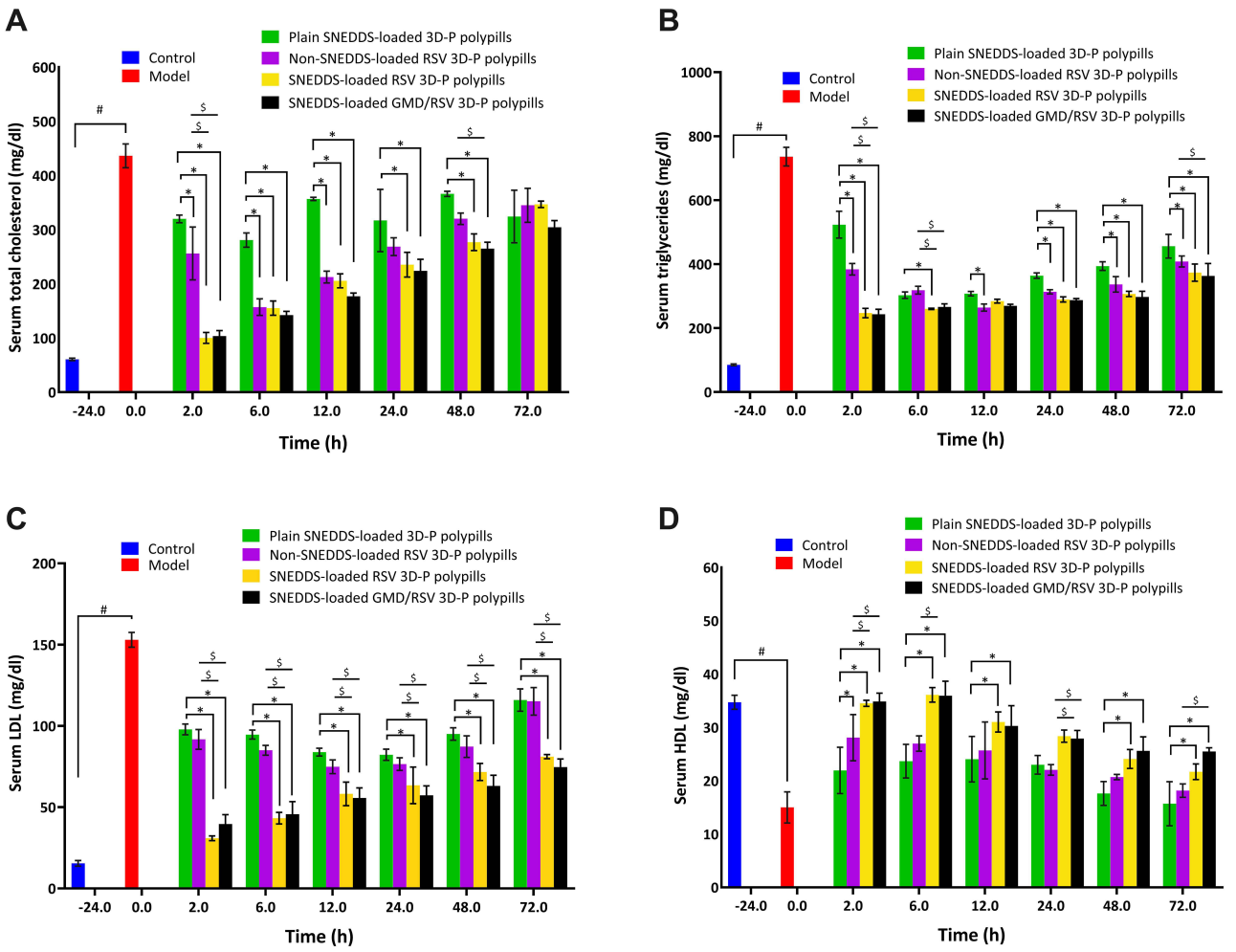

Figure 3 Serum lipid profile in induced-hyperglycemic/dyslipidemic male Wistar rats after oral treatment with a single dose of the prepared 3D-printed polypills. (**A**) Levels of total cholesterol; (**B**) levels of triglycerides; (**C**) LDL levels and (**D**) HDL levels.
Notes: #Indicates significant from the control group. *Indicates significant from plain SNEDDS-loaded 3D-P pills. $Indicates significant from non-SNEDDS-loaded 3D-P pills. Significant difference was considered at $P < 0.05$. Data are presented as mean ± SD, (n = 3).

the corresponding plain SNEDDS and the control ($P < 0.05$). Also, Figure 3B displays the level of triglycerides in the model group was significantly higher than that in the control group ($P < 0.05$). The marked reduction in the level of triglyceride was observed in all groups after 2 h and extended for 72 h. A significant reduction was noticed between the Curcuma oil-loaded SNEDDS and the SNEDDS-loaded RSV at all time points, but the significant difference was achieved only at 6 h between the non-SNEDDS loaded RSV pills and the SNEDDS-loaded RSV pills. An interesting finding by reducing the level of the circulating triglyceride was 60% after 24 h with the SNEDDS-loaded RSV 3D-P pills. These results implied that SNEDDS-loaded RSV 3D-P polypills have the potential in reducing the lipid contents in the serum of dyslipidemic rats. Similarly, serum lipoproteins were also evaluated and presented in Figure 3C and D. The LDL levels were decreased in the serum of the dyslipidemic rats treated with SNEDDS-loaded RSV 3D-P pills and SNEDDS-loaded GMD/RSV 3D-P polypills with 58.5% and 62.5%, respectively, compared with the model group after 24 h. Figure 3C reveals that there is a significant reduction ($p < 0.05$) in the LDL percentage over 72 h between the plain SNEDDS and non-SNEDDS-loaded RSV pills and the SNEDDS-loaded RSV pills. On the other hand, the plain SNEDDS-loaded 3D-P pills showed an elevated percentage in the circulating HDL by ~53% in comparison with its value in the model group. Also, it was noticed that there is no significant difference between these pills and the non-SNEDDS-loaded RSV 3D-P pills in the elevation percentage of HDL at the same time. But the significant difference has been verified between these two pills and the SNEDDS-loaded RSV and SNEDDS-loaded GMD/RSV 3D-P pills which

produced an elevation percentage of ~89%, and ~86%, respectively. Surprisingly, the level of HDL elevation reached the normal level after 2 h with significant ($p < 0.05$) elevation at all time points of the study between and the SNEDDS-loaded RSV and SNEDDS-loaded GMD/RSV 3D-P pills and the model group. The greater hypolipidemic activity of SNEDDS-loaded RSV 3D-P polypills can be explained by the greater solubilization of RSV, which could have increased absorption and thereby a higher plasma drug concentration (higher bioavailability) corresponding to the pharmacokinetic data. These findings were in good agreement with a previous work that reported an increase in HDL levels after 24 h and a reduction in the total cholesterol and LDL levels following administration of RSV solid lipid nanoparticle formulation, after 36 and 12 h, respectively.[39] Figure 4 shows the calculated atherosclerotic index (AI) as a predictor of metabolic disorders for all groups. AI was determined according to the reported formula, log (Triglyceride/HDL).[40,41] The figure displayed a significant decrease in the AI value between all formulations and the model group ($P < 0.05$). Furthermore, higher significances were observed between SNEDDS-loaded RSV pills and non-SNEDDS and plain SNEDDS formulations. These outcomes suggested that RSV-loaded SNEDDS could decrease the risk of coronary disease and atherosclerosis by boosting the level of HDL and lowering both triglyceride and LDL levels.

Assessment of Hepatoprotective and Antioxidant Activity

The most common hepatic serum biomarkers namely, AST, ALT, and ALP showed a dramatic increase after administration of poloxamer 407 in the induced-dyslipidemic rats (model) that may cause liver injury. Figures 5A–C described the significant increase ($P < 0.05$) in the level of these liver enzymes in the model group in comparison with the control one. Markedly, the rats who administered either SNEDDS-loaded RSV 3D-P pills or SNEDDS-loaded GMD/RSV 3D-P pills exerted a significant improvement ($P < 0.05$) in these parameters when compared to the groups given the non-SNEDDS-loaded GMD or RSV 3D-P pills indicating the impact of incorporating these drugs in SNEDDS formulations on their efficacy. Despite the significant reduction in the level of the AST and ALT after administration of SNEDDS-

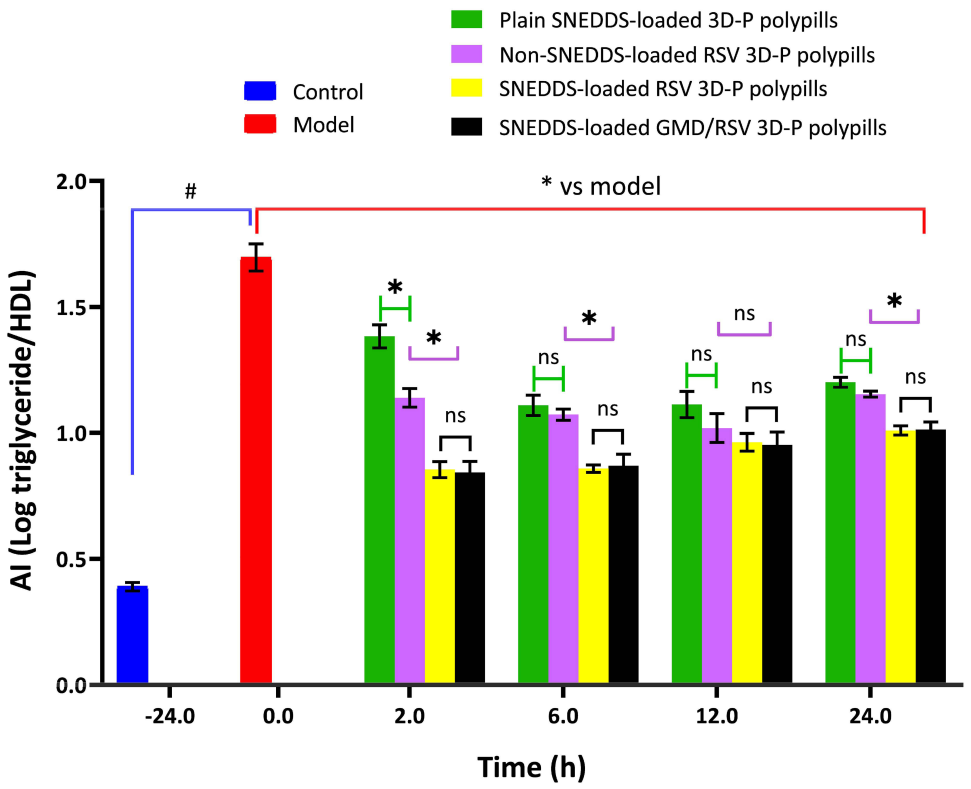

Figure 4 Atherosclerosis index of induced hyperglycemic/dyslipidemic male Wistar rats after oral administration of a single dose of the prepared 3D-printed polypills.
Notes: #Indicates significant from the control group. *Indicates significant from the model group. nsIndicates nonsignificant from the assigned groups. Significant difference was considered at $P < 0.05$. Data are presented as mean ± SD, (n = 3). Data are presented as mean ± SEM, (n = 3). Significant difference was considered at $P<0.05$.

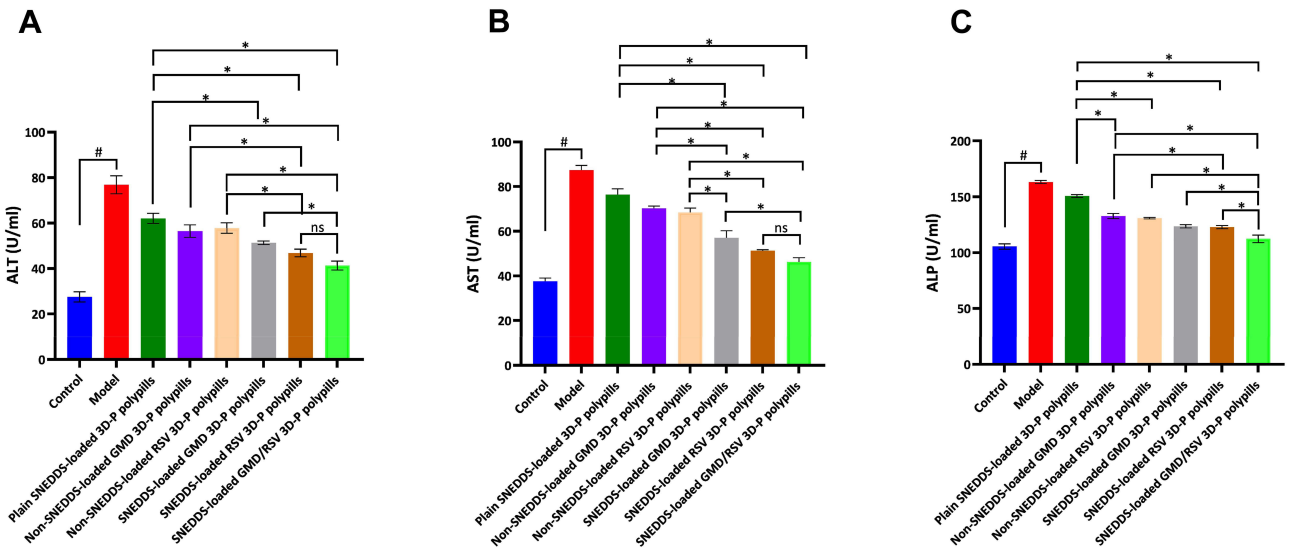

Figure 5 Serum liver enzymes (**A**) levels of ALT, (**B**) levels of AST and (**C**) levels of ALP of induced-hyperglycemic/dyslipidemic male Wistar rats after oral treatment with a single dose of the prepared 3D-printed polypills.
Notes: #Indicates significant from the control group. *Indicates significant between other groups. nsIndicates nonsignificant from the assigned groups. Significant difference was considered at $P < 0.05$. Data are presented as mean ± SD (n = 3).

loaded RSV 3D-P pills or SNEDDS-loaded GMD/RSV 3D-P pills, the figure showed that there is no significant reduction between both groups except in the ALP level. Also, the figure revealed there is a significant difference between the rats who received plain SNEDDS 3D-P pills containing only Curcuma oil and the rats who received all formulations containing GMD, RSV, or both which confirm the potential of this combination in the hepatoprotective effect. Metabolic disorders and altered liver enzymes are related to the progression of diseases like myocardial lipidosis and profound toxicity.[42]

It was recently reported that RSV has an anti-inflammatory and antioxidant effect against Poloxamer 407-induced oxidative damage.[43] As shown in Figure 6A–C a dramatic decrease with significant effect ($P < 0.05$) in the serum CAT, SOD, and GST levels, in response to Poloxamer 407 intoxication, indicated the presence of oxidative stress. Along with these data, the values of CAT, SOD, and GST that were increased following administration of the SNEDDS-loaded RSV

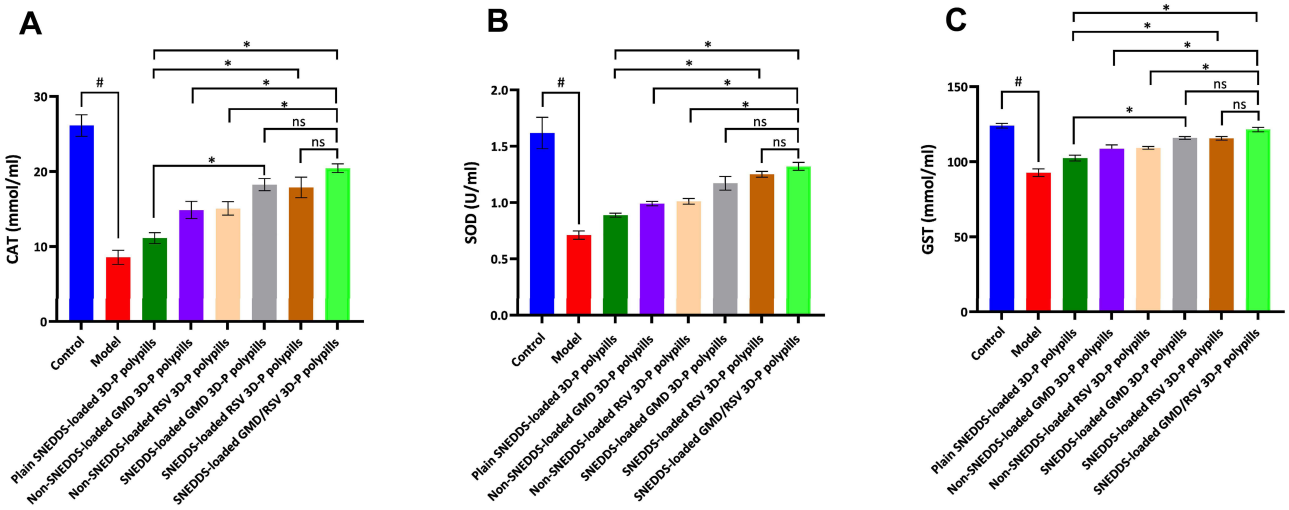

Figure 6 Antioxidant enzymes of induced-hyperglycemic/dyslipidemic male Wistar rats after oral treatment with a single dose of the prepared 3D-printed polypills. Serum levels of (**A**) CAT, (**B**) SOD, and (**C**) GST.
Notes: #Indicates significant from the control group. *Indicates significant between other groups. nsIndicates nonsignificant from the assigned groups. Significant difference was considered at $P < 0.05$. Data are presented as mean ± SD (n = 3).

3D-P pills or SNEDDS-loaded GMD/RSV 3D-P pills were closer to the control values. Notably, rats treated with SNEDDS-loaded GMD/RSV 3D-P pills significantly upregulated the antioxidant enzymes, CAT, SOD, and GST compared to the plain SNEDDS and non-SNEDDS loaded GMD or RSV ($P < 0.05$). These results support the protective effects of SNEDDS-loaded GMD/RSV 3D-P pills against Poloxamer 407-induced oxidative damage. Furthermore, by comparing the liver functions and oxidative stress in both non-SNEDDS-treated hyperglycemic/dyslipidemic and SNEDDS-treated hyperglycemic/dyslipidemic groups, we found that SNEDDS-loaded GMD/RSV 3D-P polypills had a significantly prominent reduction in serum ALT, AST, ALP levels as well as profound elevation in serum CAT, SOD, and GST levels ($P < 0.05$).

Histopathological Examination

Microscopic examination of pancreas tissues of the control group (Figure 7A) revealed the normal structure of both exocrine units and endocrine components. Islets of Langerhans appeared of normal size and contained β-cells. Pancreas tissues of the model group (Figure 7B) showed atrophied ill-distinct islets of Langerhans that contained few vacuolated and necrotic β-cells. Necrosis of islets of Langerhans was noticed accompanied by eosinophilic tissue debris. Examination of group 2 (Figure 7C) that was administered the plain SNEDDS loaded with Curcuma oil 3D-P pills revealed mild to moderate atrophy of islets of Langerhans associated with necrobiotic changes that affected some islets which characterized by vacuolation of β-cells and few necrotic debris. Administration of non-SNEDDS-loaded GMD 3D-P pills to the rats (Figure 7D) showed partial improvement in the islets of Langerhans that characterized by the presence of variable-sized islets and the existence of vacuolated cells. Regarding rats receiving non-SNEDDS-loaded RSV 3D-P pills (Figure 7E), marked vacuolation of the islets of Langerhans cells was frequently observed along with cystic dilated intralobular pancreatic ducts were commonly detected in some

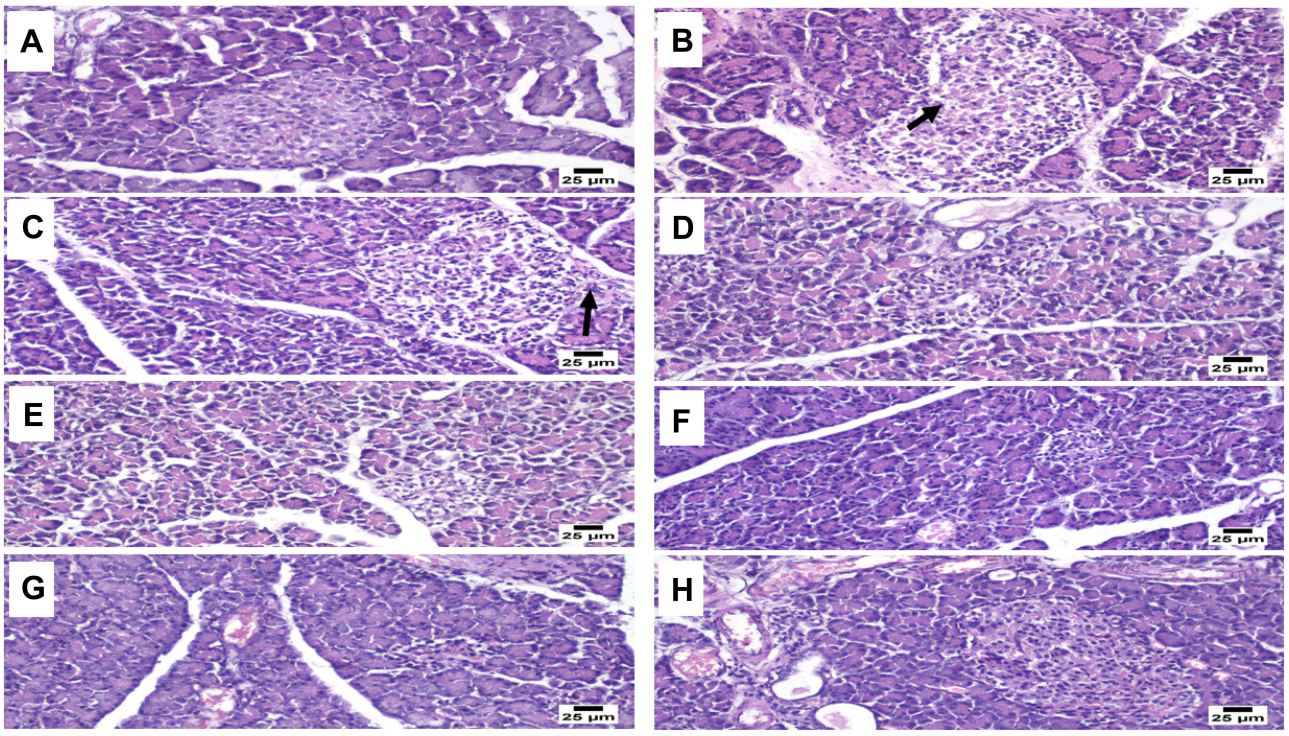

Figure 7 Histopathological images of the pancreas cells. Photomicrograph for the pancreas of the control group showing normal islets of Langerhans (**A**). Photomicrograph for the pancreas of the model group showing necrosis of islets of Langerhans admixed with an accumulation of eosinophilic tissue debris "black arrow" (**B**). Photomicrograph for the pancreas of plain SNEDDS-loaded 3D-P pills showing average-sized islets of Langerhans with few vacuolated cells (arrow) and few necrotic debris (**C**). Photomicrograph for the pancreas of non-SNEDDS-loaded GMD 3D-P pills showing vacuolation in the islets cells (**D**). Photomicrograph for the pancreas of non-SNEDDS-loaded RSV 3D-P pills showing marked vacuolation of islets cells with reduction of islets size (**E**). Photomicrograph for the pancreas of SNEDDS-loaded GMD 3D-P pills showing atrophy of pancreatic islet with vacuolation and mild congested blood vessel (**F**). Photomicrograph for the pancreas of SNEDDS-loaded RSV 3D-P pills showing mild atrophy of pancreatic islets (**G**). Photomicrograph for the pancreas of SNEDDS-loaded GMD/RSV 3D-P polypills showing apparently normal pancreatic islet (**H**).

examined sections. Administration of SNEDDS-loaded GMD 3D-P pills to animals demonstrated partial protection of the pancreatic islets that showed variable size and vacuolation of the endocrine cells (Figure 7F). A variable number of congested blood vessels was noticed in some affected tissue sections. Animals that received SNEDDS-loaded RSV 3D-P pills showed marked improvement in the pancreatic islets regarding size. However, vacuolated cells were still noticed among the examined pancreatic islets (Figure 7G). The highest protection was noticed in animals that were treated with SNEDDS-loaded GMD/RSV 3D-P polypills. The pancreatic islets of this group showed normal size with apparently normal pancreatic parenchyma including exocrine acini and pancreatic duct (Figure 7H).

As illustrated in Figure 8, the area of islets of Langerhans was decreased significantly in the model group when compared to the control group, all groups treated with SNEDDS-loaded formulations. The absence of significant difference was noticed between these groups and the highest pancreatic islets area average was noticed in the rats treated with SNEDDS-loaded GMD/RSV 3D-P polypills.

On the other hand, microscopic examination of liver tissues of the control group revealed normal hepatocytes that orderly arranged in normal lobular architecture with central veins and radiating hepatic cords. The portal triads showed normal histology containing branches of the hepatic artery, portal vein, and bile duct (Figure 9A). Animals of the model group showed diffuse steatosis of the hepatic parenchyma. The hepatocytes showed macro and microvesicular steatosis. The cytoplasm displayed a fat globule that pushed the nucleus to the periphery giving the characteristic signet ring appearance. Some examined sections showed diffuse hemorrhages and widening of hepatic sinusoids. Activation of Kupffer cells was also observed among the affected hepatic lobules associated with sporadic cell necrosis and apoptosis of hepatocytes (Figure 9B). Administration of the plain SNEDDS loaded with Curcuma oil 3D-P pills revealed partial protection of the hepatic parenchyma. Several examined sections showed widespread microvesicular steatosis among the hepatic lobules (Figure 9C). Mild improvement was recorded in rats that received non-SNEDDS-loaded GMD tablets. The hepatic parenchyma showed diffuse steatosis in the hepatocytes associated with hemorrhages and expansion of hepatic sinusoids in some instances (Figure 9D). Likewise, animals treated with non-SNEDDS-loaded RSV 3D-P pills

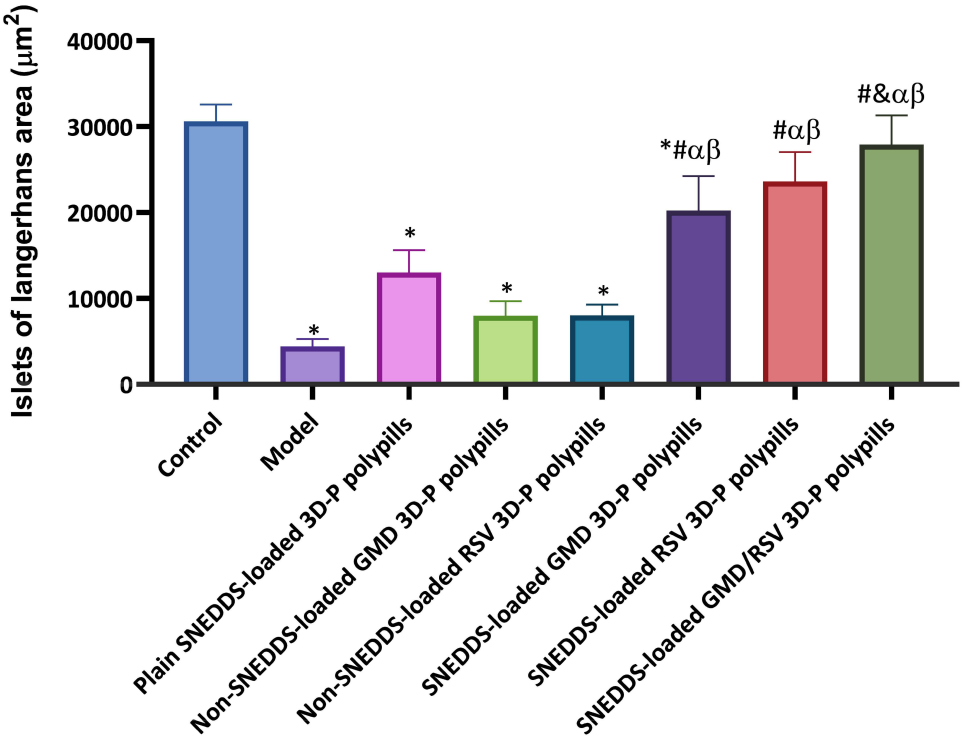

Figure 8 Area of islets of Langerhans in different groups.

Notes: *Indicates significant from the control group. #Indicates significant from the model. &Indicates significant from plain-SNEDDS-loaded 3D-P polypills. αIndicates significant from non-SNEDDS-loaded GMD 3D-P polypills. βIndicates significant from non-SNEDDS-loaded RSV 3D-P polypills. Data were presented as mean ±SD (n = 3). Significant difference was considered at $P < 0.05$.

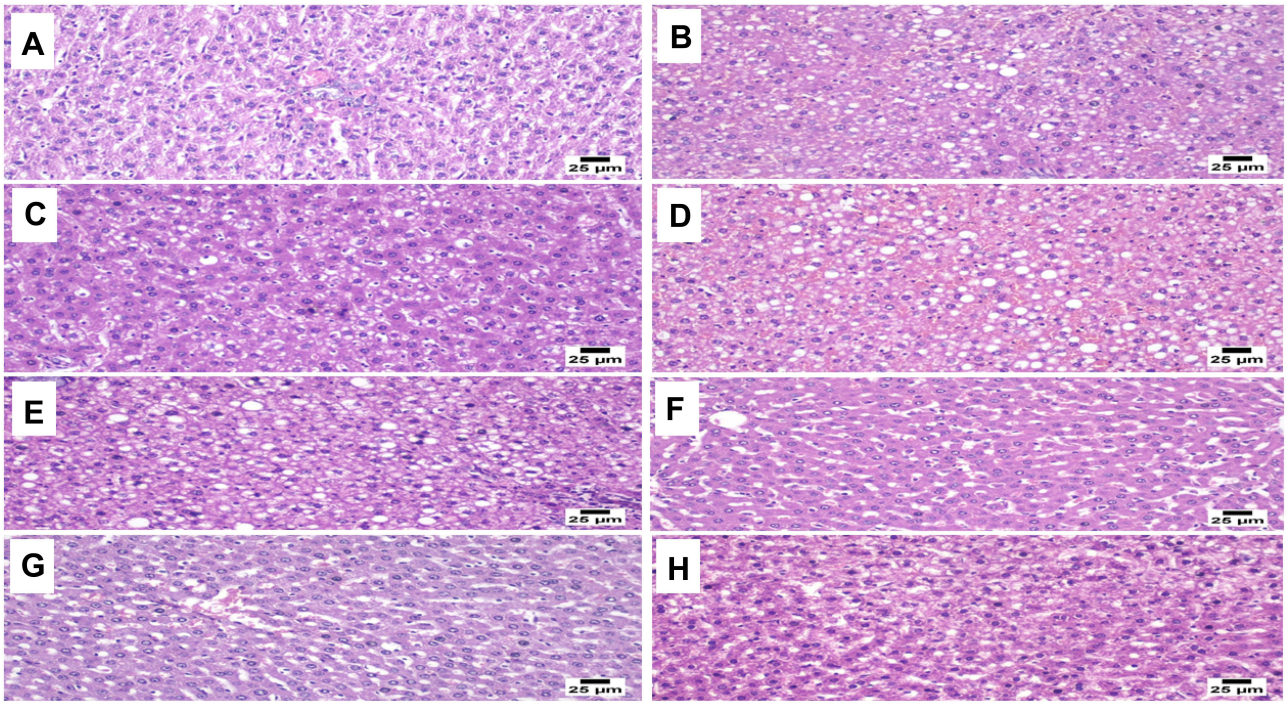

Figure 9 Histopathological images of the liver cells. Liver tissue from the control group showing normal histological structure (**A**). Liver tissue from the model group showing diffuse steatosis of the hepatic parenchyma (**B**). Liver tissue from plain-SNEDDS-loaded 3D-P polypills showing steatosis of hepatocytes (**C**). Liver tissue from non-SNEDDS-loaded GMD 3D-P polypills showing hemorrhages and steatosis of the hepatic parenchyma (**D**). Liver tissue from non-SNEDDS-loaded RSV 3D-P polypills showing widespread micro and macrovesicular steatosis in the hepatic parenchyma (**E**). Liver tissue from SNEDDS-loaded GMD 3D-P polypills showing apparently normal hepatocytes (**F**). Liver tissue from SNEDDS-loaded RSV 3D-P polypills showing mild dilation of hepatic sinusoids (**G**). Liver tissue from SNEDDS-loaded GMD/RSV 3D-P polypills showing apparently normal hepatic parenchyma (**H**).

showed marked fatty change of the affected hepatocytes associated with activation of Kupffer cells. The hepatocytes displayed large fat globules that pushed the nucleus to the periphery with a signet ring appearance (Figure 9E). Marked protection of hepatic parenchyma was noticed in rats that were administered SNEDDS-loaded GMD 3D-P pills. Examination of hepatic tissue showed apparently normal hepatocytes. However, widening of hepatic sinusoids was commonly detected in the affected tissue (Figure 9F). Similarly, SNEDDS-loaded RSV 3D-P pills administered to rats showed a marked enhancement in the hepatic parenchyma in several examined sections. The hepatic sinusoids were less expanded when compared to the group that received the SNEDDS-loaded GMD 3D-P pills. The hepatocytes appeared apparently normal with the absence of fat vacuoles in their cytoplasm (Figure 9G). Finally, examination of liver sections of animals that received SNEDDS-loaded GMD/RSV 3D-P pills showed apparently normal hepatocytes with normal hepatic sinusoids. This group illustrated the highest protection level with less detectable steatosis in the examined hepatocytes (Figure 9H). According to the studied steatosis score, a significant decrease was detected in the rats that received the plain SNEDDS loaded with Curcuma oil 3D-P pills as well as the groups that administered SNEDDS-loaded GMD, RSV, or both when compared with the model group. Meanwhile, a significant increase was recorded in the model, and groups received non-SNEDDS-loaded GMD or RSV 3D-P pills. These findings confirm the potential of Curcuma oil as adjunct therapy with GMD and RSV in the prophylaxis of steatosis in patients with metabolic disorders. The lowest level was detected in rats treated with SNEDDS-loaded RSV alone or GMD/RSV polypills which showed an absence of significant difference when compared with the control group (Figure 10).

Conclusions

Three-dimensional printing of polypills based on the Curcuma oil self-nanoemulsifying drug delivery system and loaded with glimepiride and rosuvastatin were developed and showed acceptable quality attributes. These polypills improved the pharmacokinetics of both glimepiride and rosuvastatin with $AUC_{0\text{-}t}$ values of 16,035.25 ng/mL×h and 67,811.75 ng/mL×h,

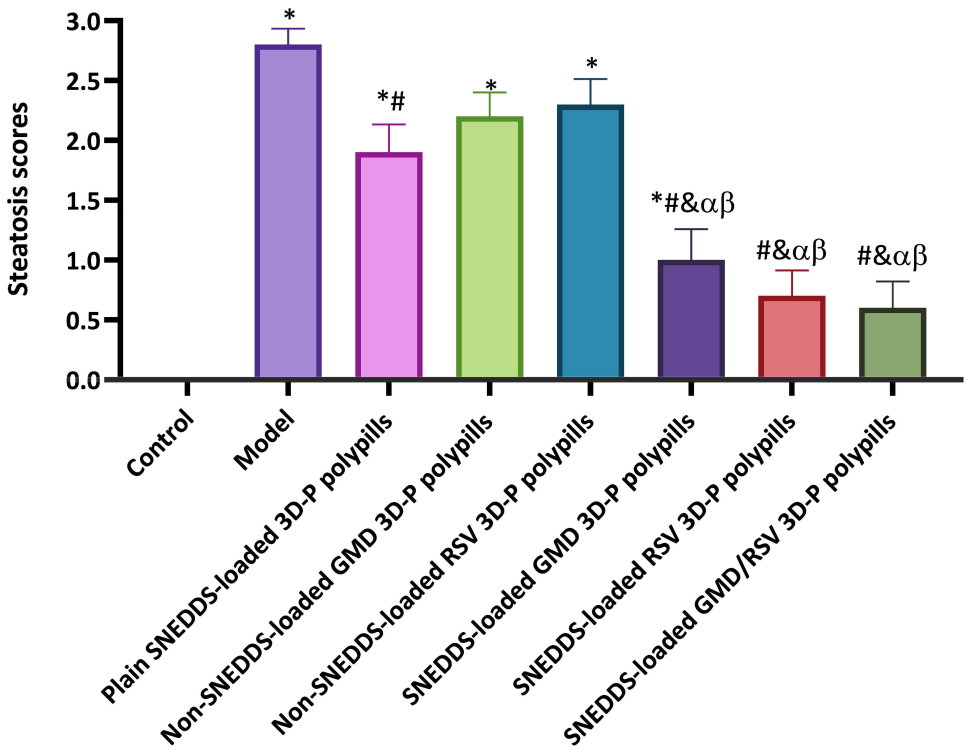

Figure 10 Liver steatosis lesion scores in different groups. Values were expressed as means ± SE.
Notes: *Indicates significant from control. #Indicates significant from the model. &Indicates significant from plain-SNEDDS-loaded 3D-P polypills. αIndicates significant from non-SNEDDS-loaded GMD 3D-P polypills. βIndicates significant from non-SNEDDS-loaded RSV 3D-P polypills. Data were presented as mean ±SD (n = 3). Significant difference was considered at $P < 0.05$.

respectively in comparison to the non-SNEDDS-loaded 3D-P pills. Furthermore, these polypills showed significant anti-dyslipidemic, hepatoprotective and antioxidant activities when compared with the control and non-SNEDDS-loaded drugs. Also, SNEDDS-loaded GMD/RSV polypills could decrease the risk of coronary disease and atherosclerosis by boosting the level of HDL and lowering both triglyceride and LDL levels. No marked hepatic histopathological changes with normal hepatic sinusoids and illustrated the highest protection level with less detectable steatosis in the examined hepatocytes. Also, microscopic examination of the pancreatic specimen showed apparently normal size pancreatic islets with apparently normal pancreatic parenchyma including exocrine acini and pancreatic duct. All these findings confirm the potential of Curcuma oil as adjunct therapy with GMD and RSV in the prophylaxis of the risk of coronary disease and liver steatosis in patients with metabolic syndrome. Further clinical studies to substantiate the present findings is needed.

Acknowledgments

The authors extend their appreciation to the Deputyship for Research & Innovation, Ministry of Education in Saudi Arabia for funding this research work through the project number "IFPRC-176-166-2020" and King Abdulaziz University, DSR, Jeddah, Saudi Arabia.

Disclosure

The authors report no conflicts of interest for this work.

References

1. O'Neill S, O'Driscoll L. Metabolic syndrome: a closer look at the growing epidemic and its associated pathologies. *Obes Rev.* 2015;16(1):1–12. doi:10.1111/obr.12229
2. Do Vale Moreira NC, Hussain A, Bhowmik B, et al. Prevalence of metabolic syndrome by different definitions, and its association with type 2 diabetes, pre-diabetes, and cardiovascular disease risk in Brazil. *Diabetes Metab Syndr Clin Res Rev.* 2020;14(5):1217–1224. doi:10.1016/j.dsx.2020.05.043

3. Ranasinghe P, Mathangasinghe Y, Jayawardena R, Hills AP, Misra A. Prevalence and trends of metabolic syndrome among adults in the Asia-pacific region: a systematic review. *BMC Public Health*. 2017;17(1):1–9. doi:10.1186/s12889-017-4041-1
4. Friend A, Craig L, Turner S. The prevalence of metabolic syndrome in children: a systematic review of the literature. *Metab Syndr Relat Disord*. 2013;11(2):71–80. doi:10.1089/met.2012.0122
5. Li X, Cao C, Tang X, et al. Prevalence of metabolic syndrome and its determinants in newly-diagnosed adult-onset diabetes in china: a multi-center, cross-sectional survey. *Front Endocrinol (Lausanne)*. 2019;10:1–9. doi:10.3389/fendo.2019.00661
6. Yadav D, Mahajan S, Subramanian SK, Bisen PS, Chung CH, Prasad GB. Prevalence of metabolic syndrome in type 2 diabetes mellitus using NCEP-ATPIII, IDF and WHO definition and its agreement in Gwalior Chambal region of Central India. *Glob J Health Sci*. 2013;5(6):142–155. doi:10.5539/gjhs.v5n6p142
7. Al-Rubeaan K, Bawazeer N, Al Farsi Y, et al. Prevalence of metabolic syndrome in Saudi Arabia - a cross sectional study. *BMC Endocr Disord*. 2018;18(1):1–9. doi:10.1186/s12902-018-0244-4
8. Naghipour M, Joukar F, Nikbakht HA, et al. High prevalence of metabolic syndrome and its related demographic factors in north of Iran: results from the PERSIAN guilan cohort study. *Int J Endocrinol*. 2021;2021:1–9. doi:10.1155/2021/8862456
9. US Department of Health and Human Services. National diabetes statistics report, 2020. Natl Diabetes Stat Rep; 2020:1–30.
10. DeBoer MD, Filipp SL, Gurka MJ. Use of a metabolic syndrome severity z score to track risk during treatment of prediabetes: an analysis of the diabetes prevention program. *Diabetes Care*. 2018;41(11):2421–2430. doi:10.2337/dc18-1079
11. Belete R, Ataro Z, Abdu A, Sheleme M. Global prevalence of metabolic syndrome among patients with type I diabetes mellitus: a systematic review and meta-analysis. *Diabetol Metab Syndr*. 2021;13(1):1–13. doi:10.1186/s13098-021-00641-8
12. Arefian M, Mirzaei M, Eshtiagh-Hosseini H, Frontera A. A survey of the different roles of polyoxometalates in their interaction with amino acids, peptides and proteins. *Dalt Trans*. 2017;46(21):6812–6829. doi:10.1039/C7DT00894E
13. Alizadeh H, Mirzaei M, Saljooghi AS, et al. Coordination complexes of zinc and manganese based on pyridine-2,5-dicarboxylic acid N -oxide: DFT studies and antiproliferative activities consideration. *RSC Adv*. 2021;11(59):37403–37412. doi:10.1039/D1RA08258B
14. Moradi HS, Momenzadeh E, Asar M, et al. Bioactivity studies of two copper complexes based on pyridinedicarboxylic acid N-oxide and 2,2′-bipyridine. *J Mol Struct*. 2022;1249:131584. doi:10.1016/J.MOLSTRUC.2021.131584
15. Sabouri Z, Sabouri M, Amiri MS, Khatami M, Darroudi M. Plant-based synthesis of cerium oxide nanoparticles using Rheum turkestanicum extract and evaluation of their cytotoxicity and photocatalytic properties. *Mater Technol*. 2020;1–14. doi:10.1080/10667857.2020.1863573
16. Charbgoo F, Bin AM, Darroudi M. Cerium oxide nanoparticles: green synthesis and biological applications. *Int J Nanomedicine*. 2017;12:1401–1413. doi:10.2147/IJN.S124855
17. Ashraf J, Mughal EU, Alsantali RI, et al. 2-Benzylidenebenzofuran-3(2 H)-ones as a new class of alkaline phosphatase inhibitors: synthesis, SAR analysis, enzyme inhibitory kinetics and computational studies. *RSC Adv*. 2021;11(56):35077–35092. doi:10.1039/D1RA07379F
18. Hashemzadeh A, Drummen GPC, Avan A, et al. When metal–organic framework mediated smart drug delivery meets gastrointestinal cancers. *J Mater Chem B*. 2021;9(19):3967–3982. doi:10.1039/D1TB00155H
19. Pivari F, Mingione A, Brasacchio C, Soldati L. Curcumin and type 2 diabetes mellitus: prevention and treatment. *Nutrients*. 2019;11(8):1837. doi:10.3390/nu11081837
20. Kim M, Kim Y. Hypocholesterolemic effects of curcumin via up-regulation of cholesterol 7a-hydroxylase in rats fed a high fat diet. *Nutr Res Pract*. 2010;4(3):191. doi:10.4162/nrp.2010.4.3.191
21. Rivera-Mancía S, Trujillo J, Chaverri JP. Utility of curcumin for the treatment of diabetes mellitus: evidence from preclinical and clinical studies. *J Nutr Intermed Metab*. 2018;14:29–41. doi:10.1016/j.jnim.2018.05.001
22. Sahebkar A, Saboni N, Pirro M, Banach M. Curcumin: an effective adjunct in patients with statin-associated muscle symptoms? *J Cachexia Sarcopenia Muscle*. 2017;8(1):19–24. doi:10.1002/jcsm.12140
23. Marton LT, Pescinini-e-Salzedas LM, Camargo MEC, et al. The effects of curcumin on diabetes mellitus: a systematic review. *Front Endocrinol*. 2021;12. doi:10.3389/fendo.2021.669448
24. Vogenberg FR, Barash CI, Pursel M. Personalized medicine - Part 1: evolution and development into theranostics. *P T*. 2010;35(10):560–567.
25. Lesko LJ. Personalized medicine: elusive dream or imminent reality? *Clin Pharmacol Ther*. 2007;81(6):807–816. doi:10.1038/sj.clpt.6100204
26. Ahmed TA, Felimban RI, Tayeb HH, et al. Development of multi-compartment 3d-printed tablets loaded with self-nanoemulsified formulations of various drugs: a new strategy for personalized medicine. *Pharmaceutics*. 2021;13(10):1733. doi:10.3390/pharmaceutics13101733
27. USP 41-NF 36. The United States pharmacopeia national formulary. Twinbrook Parkway, Rockville, MD: The United States Pharmacopeial Convention; 2018.
28. Ahmed OAA, Ahmed TA, Abdel-naim AB, Khedr A, Banjar ZM, Afouna MI. Enhancement of in vitro skin transport and in vivo hypoglycemic efficacy of glimepiride transdermal patches. *Trop J Pharm Res*. 2014;13(8):1207–1213. doi:10.4314/tjpr.v13i8.3
29. Ahmed TA, Elimam H, Alrifai AO, et al. Rosuvastatin lyophilized tablets loaded with flexible chitosomes for improved drug bioavailability, anti-hyperlipidemic and anti-oxidant activity. *Int J Pharm*. 2020;588:119791. doi:10.1016/j.ijpharm.2020.119791
30. Mahajan TC, Deshmukh SB, Badgujar VL, Chhajed PN, Patil JA. RP-HPLC method development and validation for estimation of metformin, voglibose, glimepiride in bulk and combined tablet dosage forms. *Int J Chem Pharm Sci*. 2016;4(12):697–702.
31. El-Say KM, Ahmed TA, Aljefri AH, El-Sawy HS, Fassihi R, Abou-Gharbia M. Oleic acid–reinforced PEGylated polymethacrylate transdermal film with enhanced antidyslipidemic activity and bioavailability of atorvastatin: a mechanistic ex-vivo/in-vivo analysis. *Int J Pharm*. 2021;608:121057. doi:10.1016/j.ijpharm.2021.121057
32. Brunt EM, Janney CG, Di Bisceglie AM, et al. Nonalcoholic steatohepatitis: a proposal for grading and staging the histological lesions. *Am J Gastroenterol*. 1999;94(9):2467–2474. doi:10.1111/J.1572-0241.1999.01377.X
33. Godfrey KR, Arundel PA, Dong Z, Bryant R. *Modelling the Double Peak Phenomenon in Pharmacokinetics*. IFAC; Vol. 42, 2009. doi:10.3182/20090812-3-DK-2006.0001
34. Wu W, Wang Y, Que L. Enhanced bioavailability of silymarin by self-microemulsifying drug delivery system. *Eur J Pharm Biopharm*. 2006;63(3):288–294. doi:10.1016/j.ejpb.2005.12.005
35. Chang RK, Shojaei AH. Effect of a lipoidic excipient on the absorption profile of compound UK 81252 in dogs after oral administration. *J Pharm Pharm Sci*. 2004;7(1):8–12.

36. Al-Amodi YA, Hosny KM, Alharbi WS, Safo MK, El-Say KM. Investigating the potential of transmucosal delivery of febuxostat from oral lyophilized tablets loaded with a self-nanoemulsifying delivery system. *Pharmaceutics*. 2020;12(534):1–18. doi:10.3390/pharmaceutics12060534
37. El-Say KM, Ahmed TAA, Ahmed OAA, Elimam H. Enhancing the hypolipidemic effect of simvastatin in poloxamer-induced hyperlipidemic rats via liquisolid approach: pharmacokinetic and pharmacodynamic evaluation. *AAPS PharmSciTech*. 2020;21(6):223. doi:10.1208/s12249-020-01754-5
38. El-Say KM, Ahmed TA, Ahmed OAA, Hosny KM, Abd-Allah FI. Self-nanoemulsifying lyophilized tablets for flash oral transmucosal delivery of vitamin K: development and clinical evaluation. *J Pharm Sci*. 2017;106(9):2447–2456. doi:10.1016/j.xphs.2017.01.001
39. Dudhipala N, Veerabrahma K. Improved anti-hyperlipidemic activity of Rosuvastatin Calcium via lipid nanoparticles: pharmacokinetic and pharmacodynamic evaluation. *Eur J Pharm Biopharm*. 2017;110:47–57. doi:10.1016/j.ejpb.2016.10.022
40. Dobiášová M, Frohlich J. The plasma parameter log (TG/HDL-C) as an atherogenic index: correlation with lipoprotein particle size and esterification rate inapob-lipoprotein-depleted plasma (FERHDL). *Clin Biochem*. 2001;34(7):583–588. doi:10.1016/S0009-9120(01)00263-6
41. Kanthe PS, Patil BS, Bagali S, Deshpande A, Shaikh GB, Aithala M. Atherogenic index as a predictor of cardiovascular risk among women with different grades of obesity. *Int J Collab Res Intern Med Public Heal*. 2012;4(10):1767–1774.
42. Hasan KMM, Tamanna N, Haque MA. Biochemical and histopathological profiling of Wistar rat treated with Brassica napus as a supplementary feed. *Food Sci Hum Wellness*. 2018;7(1):77–82. doi:10.1016/j.fshw.2017.12.002
43. Duarte T, Da Cruz IBM, Barbisan F, Capelleto D, Moresco RN, Duarte MMMF. The effects of rosuvastatin on lipid-lowering, inflammatory, antioxidant and fibrinolytics blood biomarkers are influenced by Val16Ala superoxide dismutase manganese-dependent gene polymorphism. *Pharmacogenomics J*. 2016;16(6):501–506. doi:10.1038/tpj.2015.91